

# Propagation of wave modes and antispiral waves in a reaction-diffusion system

Chen Wang,<sup>1</sup> ChunXia Zhang,<sup>1</sup> and Qi Ouyang<sup>1,2,3,\*</sup><sup>1</sup>*Department of Physics, Peking University, Beijing 100871, People's Republic of China*<sup>2</sup>*Center for Theoretical Biology, Peking University, Beijing 100871, People's Republic of China*<sup>3</sup>*The Beijing-Hong Kong-Singapore Joint Center for Nonlinear and Complex Systems (PKU), Peking University, Beijing 100871, People's Republic of China*

(Received 14 May 2006; published 18 September 2006)

Since the observation of antispirals by Vanag *et al.* in a reaction-diffusion system, the study of its origin becomes a focus of nonlinear science and pattern formation. It was shown that antispirals may exist in a reaction-diffusion system when the system is near the onset of Hopf bifurcation. Here, we demonstrate that antispiral waves can also exist in a relaxational oscillatory medium, which is far from Hopf onset. Furthermore, we clarify the previously unclear concept of group velocity in inharmonic nonlinear waves, and prove that the group velocity  $v_g = d\omega/dk$  is physically significant and valid both for excitable media and for oscillatory media. From this formula, we identify two types of wave propagating fronts: gentle mode front and steep mode front. Finally, we discuss the origin of counterpropagating waves and propose necessary conditions for antispiral formation. A direct deduction from these criteria is that antispirals cannot exist in an excitable medium.

DOI: [10.1103/PhysRevE.74.036208](https://doi.org/10.1103/PhysRevE.74.036208)

PACS number(s): 82.40.Bj, 82.40.Ck, 45.70.Qj, 89.75.Kd

## I. INTRODUCTION

Spiral waves have been widely observed in diverse physical, chemical, and biological systems [1,2]. During a long period of time, all the spiral waves found in experiments propagate outwards from the spiral center. However, after the recent discovery of inwardly rotating spiral waves in a BZ-AOT system [3], the mechanism of such “antispiral waves” becomes an appealing topic in the research of pattern formation [4–9]. The appearance of antispirals is due to the breakdown of classic eikonal relation; modified eikonal relation [10,11] suggests the possibility of such patterns in highly dispersive media. Two characteristics of antispirals in sharp contrast to normal spirals have been noticed: negative dispersion  $d\omega/d|k| < 0$  [12,13] and faster bulk oscillation  $\Omega_k < \Omega_0$  [3,6].

Although antispiral centers were once assumed to be sinks of inward propagating waves, it has been recently proposed that they are in fact wave sources that emit phase waves and organize the surrounding region just like those in normal spirals [5]. Analysis of the complex Ginzburg-Landau equation (CGLE) shows that the directions of the group velocity and the phase velocity of antispiral waves are opposite. So far CGLE successfully describes the properties of antispirals observed in experiments, since these kind of waves have only been observed in harmonic oscillatory regimes close to Hopf onset. When the system moves away from Hopf onset, antispirals undergo a transition to spirals with oscillation becoming inharmonic. It was even stated that antispirals can occur only near Hopf bifurcation [6].

Although antispirals were accepted as “phase waves” with substantially different group velocity and phase velocity, there is no sharp distinction between phase waves and trigger waves in reaction-diffusion media. During the transition of the two kind of waves, even the concepts of group velocity

and phase velocity become vague since the classical derivation of group velocity  $v_g = \frac{d\omega}{dk}$  is based on the linear decomposition of wave packets into sinusoidal modes [15]. In the quite limited number of documents concerning nonlinear group velocity, we find that the only velocity which has a well-defined nonlinear counterpart is the energy transport velocity [16–18]. In pattern formation, some concepts were used to implicate the spirit of group velocity, such as mean flow [19] and transportation of perturbation [5]. However, its exact form has not been mathematically developed.

In this paper, we study a modified standard model [14] of a reaction-diffusion system and find antispirals with relaxational oscillation in numeric simulation. Although the model has no correspondence in the real physical world so far, it indicates that the former hypothesis about the requirement of antispirals [6] is not necessarily correct. The detailed result is given in Sec. II. In Sec. III, we propose that the group velocity in inharmonic nonlinear waves represents the propagating velocity of wave modes (similar to what is discussed in Ref. [16]) and prove  $v_g = \frac{d\omega}{dk}$  with some presumptions. A theory of wave mode selection is derived and checked by simulations of one-dimensional (1D) waves. In Sec. IV, we discuss the origin of counterpropagating waves and propose the necessary conditions for the occurrence of antispirals.

## II. ANTISPIRALS FAR FROM OSCILLATORY ONSET

The model we used in numeric simulation is a pure theoretical model derived from the “standard model” [14] in a reaction-diffusion system. It consists of two variables,  $u$  and  $v$ . The dynamic equations are the following:

$$\frac{\partial u}{\partial t} = f(u, v) + D_u \nabla^2 u, \quad \frac{\partial v}{\partial t} = g(u, v) + D_v \nabla^2 v. \quad (1)$$

The local reaction kinetics are given by

\*Electronic address: qi@pku.edu.cn

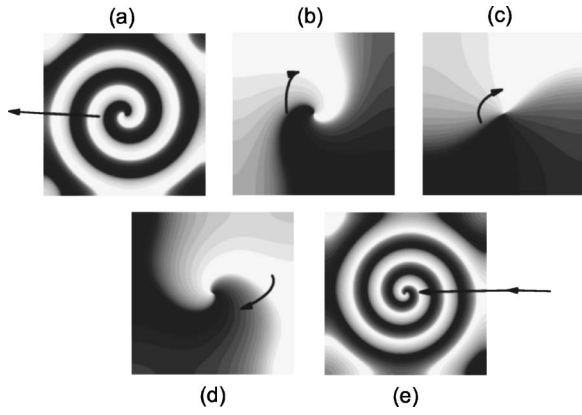


FIG. 1. Spiral-antispiral transition in models (1)–(3) with  $a=2.00$ ,  $\varepsilon=0.10$ . (a) Well-developed spiral ( $h=-0.30$ ). (b) Limited spiral ( $h=-0.10$ ). (c) Mediate status between spiral and antispiral ( $h=0.20$ ). (d) Limited antispiral ( $h=0.60$ ). (e) Well-developed antispiral ( $h=1.80$ ).

$$f(u,v) = \frac{1}{\varepsilon}(u - av - u^3)[1 + h(u^2 + v^2)], \quad (2)$$

$$g(u,v) = (u - v)[1 + h(u^2 + v^2)], \quad (3)$$

where  $a$ ,  $\varepsilon$ , and  $h$  are parameters.  $a$  controls the distance from Hopf bifurcation (the Hopf onset is at  $a=1$ ) of the fixed point ( $u_0=0, v_0=0$ );  $\varepsilon$  controls the ratio of time scales between  $u$  and  $v$ . A factor  $[1 + h(u^2 + v^2)]$  with parameter  $h$  is added to the standard model to alter the dispersion of the system. The change of  $h$  does not influence the dynamics

around the fixed point and the distance from Hopf bifurcation, but contributes considerably when variables go far from the fixed point.

The simulation is done in a two-dimensional (2D) Cartesian coordinate system with grid size  $400 \times 400$ . The simple Euler method is applied with a time step  $dt=0.005$  time unit and a space step  $dx=dy=0.2$  length unit. We choose  $h$  as the control parameter, keeping  $a=2.00$  and  $\varepsilon=0.10$  so that the system is far from Hopf onset. In these cases the oscillatory medium is highly inharmonic with big amplitude. When  $h$  is small, developing from a proper initial condition, we observe outwardly rotating spiral waves filling the space, as shown in Fig. 1(a). With the increasing of  $h$ , the wavelength of the spiral becomes longer. When  $h$  crosses a critical value  $h=-0.15$ , the organized region of the spiral core becomes so limited that it is hard to measure the wavelength of the spiral. However, the surrounding structure of the central defect point is still like an outwardly rotating spiral, as shown in Fig. 1(b). Further increasing  $h$  leads to a divergence in wavelength [Fig. 1(c)] followed by the change of wave direction [Fig. 1(d)]. Since the organized area is small, the transition from spirals to antispirals is not sharp. When  $h$  goes beyond another critical value  $h=1.10$ , the organized region of the antispiral core expands to the whole space, as shown in Fig. 1(e). The wavelength of antispiral increases with the increase of  $h$ . Figure 2(a) gives the relation between wave number and control parameter  $h$ , which shows the spiral-antispiral transition. Figures 2(b1) and 2(b2) are the time sequences of  $u$  and  $v$  at an arbitrary spatial point, from which we see relaxational oscillation with large amplitude.

Although CGLE fails in describing dynamics of relaxational oscillation, the essential characteristics of antispirals

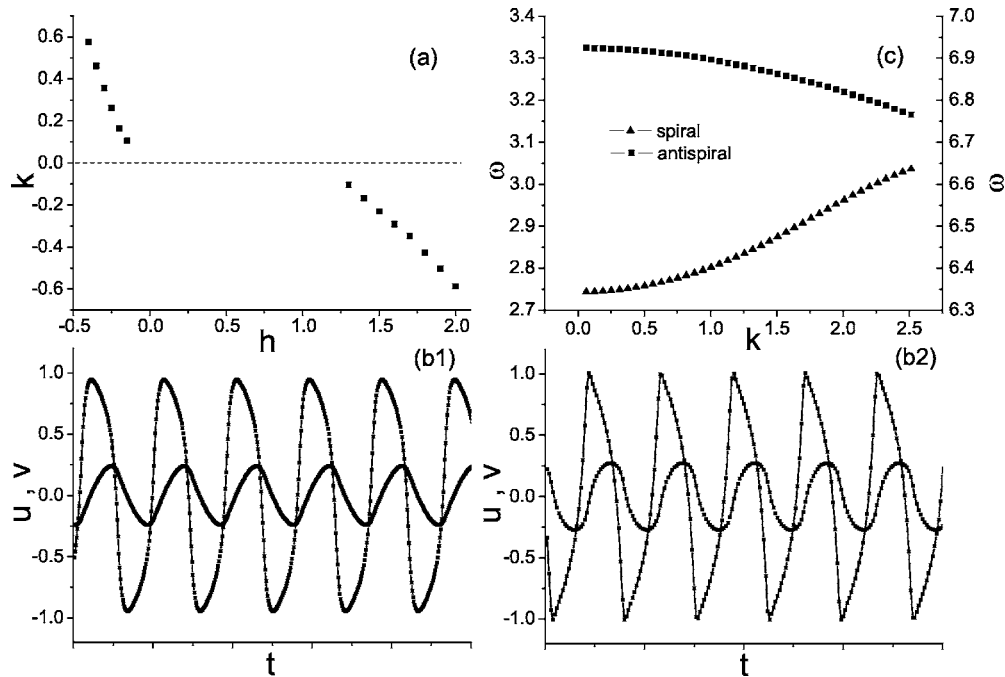


FIG. 2. Some properties of spiral and antispiral in models (1)–(3). (a) Relation between wave number and control parameter. (b1) ( $h=-0.30$ ) and (b2) ( $h=1.80$ ), oscillations of  $u$  and  $v$  at an arbitrary spatial point. The curve with larger amplitude is for  $u$ . (c) Dispersion curve of the medium for spiral ( $h=-0.30$ ) and antispiral ( $h=1.80$ ). The  $\omega$  axis on the left side is for spiral and the right one is for antispiral.

far from the Hopf onset are much the same as those near the onset. In the spiral case [Fig. 1(a)], the angular frequency of the bulk oscillation (2.743) is smaller than that of the spiral (2.750); in the antispiral case [Fig. 1(e)], the angular frequency of the bulk oscillation (6.925) is larger than that of the antispiral (6.915). In the spiral case the slope of dispersion is positive while in the antispiral case it is negative [Fig. 2(c)]. Moreover, considering the asymptotic behavior of spirals (or antispirals) as plane waves far from the core,  $\Omega_k < \Omega_0$  could be derived from  $d\omega/d|k| < 0$  and vice versa. So we conclude that the distance from Hopf onset cannot serve as the indicator of the spiral-antispiral transition, while the dispersion of the wave is more essential. The fact that antispirals have not been found far from Hopf onset only reveals that waves far from onset usually have a positive slope of dispersion.

### III. THEORY OF GROUP VELOCITY IN INHARMONIC NONLINEAR WAVES

In spite of the inward-pointing phase velocity of waves or even the inward-moving sharp wave fronts obtained in the simulation, the group velocity of waves is still pointing outwards. This is confirmed by observing that antispiral originates in the central area and gradually expands and occupies the whole space, so that we agree with the former conclusion that the phenomenon of an inward-propagating antispiral is just an illusion [5], even in cases of inharmonic oscillatory media with large oscillatory amplitude.

We define the phase velocity and group velocity of waves in inharmonic nonlinear waves under the following two assumptions: (a) during a small period of time, each spatial point oscillates with a definite mode defined by  $(k, \omega)$ , which is a point on the dispersion curve; (b) at every moment, phase of each spatial point could be defined and it is continuous in space. Then we get  $k$  (wave number),  $\omega$  (frequency), and  $\phi$  (phase) as functions of space and time.  $k$  and  $\omega$  obey the dispersion of the medium, while  $\omega = \partial\phi/\partial t$  should also be satisfied. A wave mode here is no longer a sinusoidal mode, but stands for the typical wave form with wave number  $k$  in the given point in the medium. The medium could be either oscillatory or excitable. The latter case can be considered as the limit of  $\omega_0 \rightarrow 0$ . With these presumptions, the phase velocity is defined in the traditional way as the velocity of an observer observing a fixed phase at a spatial point, while group velocity is defined as the velocity of an observer observing fixed mode (described by frequency or wave number) at a spatial point. Obviously, the phase velocity can be calculated as  $V_p = \omega/k$ .

For simplicity, we consider a 1D situation. Considering the development of a wave, we select three spatial points  $x_1, x_2, x_3$  satisfying  $x_3 - x_2 = x_2 - x_1 = \Delta x$ . The local wave number  $k$ , frequency  $f$ , and phase  $\phi$  of each point are designed in Fig. 3. It should be emphasized that  $k$  can be both positive or negative. Positive  $k$  means that  $\phi$  decreases with the increasing of  $x$  and vice versa. We let  $\Delta x$  be infinitesimally small and the oscillation modes in the area  $[x_1, x_3]$  are almost the same. Here we add an assumption that wave modes are continuous. Suppose that during a period of time  $\Delta t$ , the mode

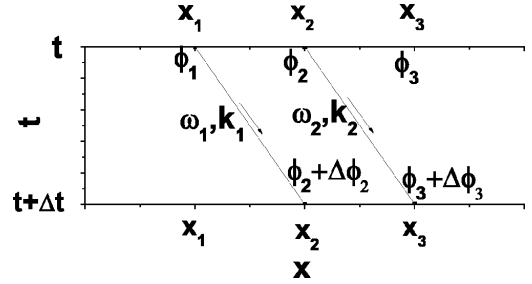


FIG. 3. A sketch map for the derivation of group velocity.

$(k_1, \omega_1)$  propagates from  $x=x_1$  to  $x=x_2$  and the mode  $(k_2, \omega_2)$  propagates from  $x=x_2$  to  $x=x_3$ . The following relations of the phases should be satisfied:

$$\phi_1 - \phi_2 = \bar{k}_{12}\Delta x, \quad \phi_2 - \phi_3 = \bar{k}_{23}\Delta x, \quad (4)$$

$$(\phi_2 + \Delta\phi_2) - (\phi_3 + \Delta\phi_3) = \bar{k}_{12}\Delta x, \quad (5)$$

$$\Delta\phi_2 = \bar{\omega}_{12}\Delta t, \quad \Delta\phi_3 = \bar{\omega}_{23}\Delta t, \quad (6)$$

where  $\bar{k}_{12}$  refers to the average wave number between  $x_1$  and  $x_2$ ;  $\bar{\omega}_{12}$  refers to the average frequency between  $x_1$  and  $x_2$ . From these equations, we get the solution of group velocity

$$V_g = \frac{\Delta x}{\Delta t} = \frac{\bar{\omega}_{12} - \bar{\omega}_{23}}{\bar{k}_{12} - \bar{k}_{23}}. \quad (7)$$

For  $\Delta x \rightarrow 0$  limit,

$$\bar{\omega}_{12} = (\omega_1 + \omega_2)/2, \quad \bar{\omega}_{23} = (\omega_2 + \omega_3)/2, \quad (8)$$

$$\bar{k}_{12} = (k_1 + k_2)/2, \quad \bar{k}_{23} = (k_2 + k_3)/2, \quad (9)$$

$$V_g = \frac{\omega_1 - \omega_3}{k_1 - k_3} = \frac{d\omega}{dk}. \quad (10)$$

As long as we get the dispersion curve of a medium, we can calculate group velocity.

We can use this result to predict the development of a new mode introduced into the medium. As a special example, we analyze 1D wave propagation under an initial condition of homogenous oscillation. Suppose at the moment  $t=0$ , the left boundary of the space was forced to oscillate with  $\omega = \omega_k$  ( $\omega$  should be within the range of dispersion curve) so that the mode  $(k, \omega_k)$  would spread into the space and replace the initial mode  $(0, \omega_0)$ . We discuss two typical types of the wave propagation in medium with positive dispersion to illustrate and validate our analysis:

(a) Gentle mode front — when  $V_g$  decreases with  $k$  as shown in Fig. 4(a). The wave front of the forced oscillation mode is characterized by a sharp variation on the  $k \sim x$  or  $\omega \sim x$  curve, as the curve 1 shown in Fig. 4(b). Since the wave front represents the front of a new mode, we will call it mode front in contrast to the traditional concept of wave front. Because the group velocity of small  $k$  or  $\omega$  is larger than that of big  $k$  or  $\omega$ , the mode front becomes increasingly plain, as the curves 2 and 3 shown in Fig. 4(b). The wave

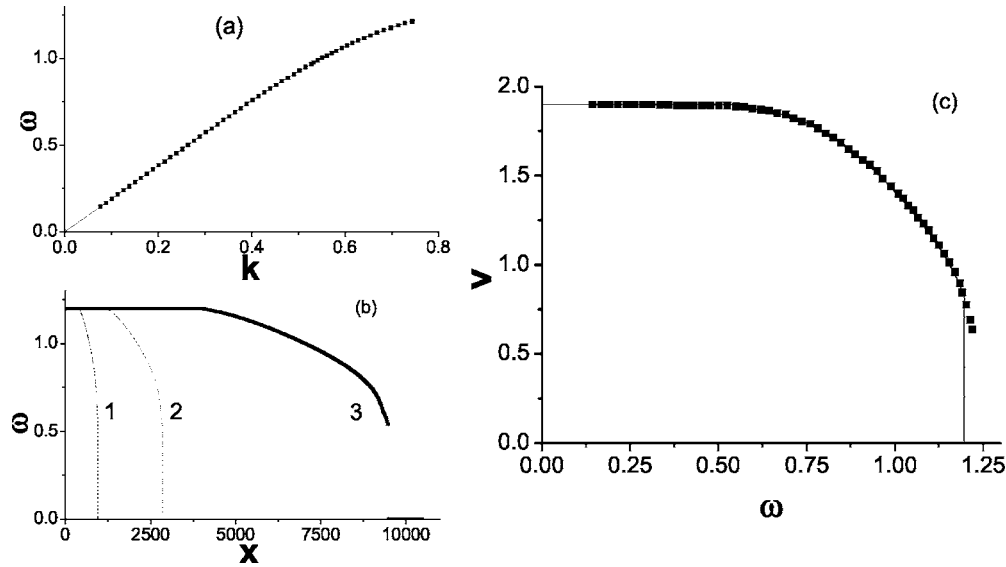


FIG. 4. Gentle mode front: the propagation of oscillatory modes in the Barkley model; parameters are  $a=0.90, b=0.10, \epsilon=0.02, D_u=1.0, D_v=0.0$ . (a) The dispersion curve shows constant group velocity for small  $k$  and decreasing group velocity for large  $k$ . (b) The spatial distribution of frequency (that indicates the propagation of wave modes) at  $t=500, 1500, 5000$  for curves 1,2,3, respectively. (c) The comparison of the propagation velocity of wave modes (described by frequency here) calculated from group velocity (triangles) and obtained from numeric simulation (the solid line).

number at each spatial point increases gradually after it receives the fastest propagating signal of small  $k$  until it is organized by the mode  $(k, \omega_k)$ .

This type of propagation could be exemplified in a typical excitable system of Barkley model [20]; the dispersion relation of the system is given in Fig. 4(a). In our 1D simulation of the model, we force the left boundary of the system to oscillate with frequency  $\omega$  ( $\omega > \omega_{kc}$ ) at  $t=0$  and monitor the wave propagating into the initially relaxed space. The  $\omega \sim x$  curves [Fig. 4(b)] calculated from the simulation results [21] represent the distribution of wave modes in the space at  $t_0=0, t_1=500, t_2=1500$ , and  $t_3=5000$ , from which we could see that the mode front is originally steep and becomes increasingly plain as it develops further. By simply dividing the traveling distance of these modes by the time consumed, we get the propagation velocity of these modes, which precisely fit the calculation of group velocity, as shown in Fig. 4(c).

(b) Steep mode front—when  $V_g$  increases with  $k$ . Because the group velocity of big  $k$  is larger than that of small  $k$ , the

mode front will become increasingly sharper until it becomes vertical. When the signal front is vertical, Eq. (10) of group velocity fails since it requires the continuation of the wave mode. However, in this condition the formulation of group velocity becomes even simpler;

$$V_g = \frac{\Delta\omega}{\Delta k}, \quad (11)$$

where  $\Delta$  means the difference between the two sides of the signal front. In other words, when the dispersion is a concave function, the group velocity is the slope of the straight line in the dispersion relation linking the two sides of the signal front, as shown in Fig. 5(a). The velocity here could also be regarded as an average value of group velocities within the range of changing of  $k$ .

The modified standard models (1)–(3) we used above is an example of this type of propagation. The dispersion relation for  $h=-0.30$  is shown in Fig. 5(a). The steep mode front

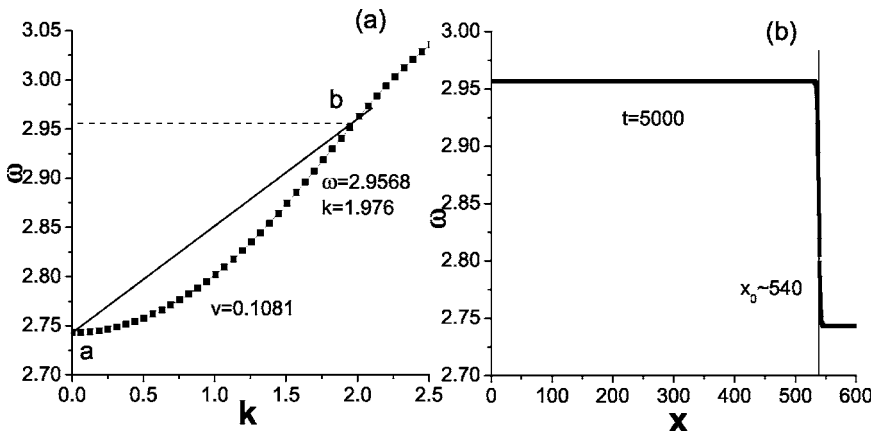


FIG. 5. Steep mode front—the propagation of oscillatory modes in models (1)–(3),  $a=2.00, \epsilon=0.10, h=-0.30$ . (a) The dispersion curve shows an increasing group velocity from point “a” to point “b”. (b) The spatial distribution of wave modes at  $t=5000$  shows a steep mode front, whose traveling velocity fit the calculation of group velocity.

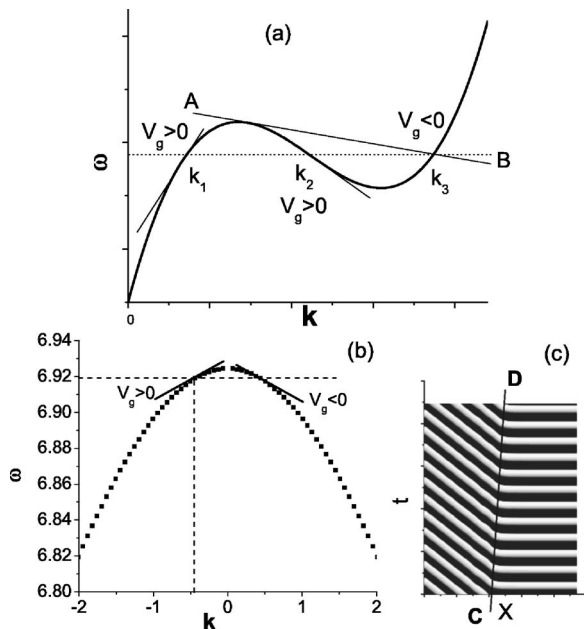


FIG. 6. Wave mode selection and counterpropagating waves. (a) A sketch map of an imaginary dispersion in which only mode  $(k_1, \omega_0)$  could be selected. (b) The complete dispersion curve of models (1)–(3) ( $a=2.00, \varepsilon=0.10, h=-0.30$ ) illustrates the selection of negative wave numbers according to group velocity judgment ( $V_g > 0$ ). (c) The time-space plot in numerical simulation shows counterpropagating waves in the same medium as (b); the slope of line CD represents the group velocity of wave modes, which is positive.

in simulation is shown in Fig. 5(b), which travels with a group velocity approximately equal to  $\Delta\omega/\Delta k=0.1081$ .

#### IV. ORIGIN OF COUNTERPROPAGATING WAVES AND ANTISPIRALS

If the dispersion curve is not monotonic, one forcing frequency  $\omega$  could correspond to several wave numbers. The system should select a mode that has a positive group velocity so that the wave pattern could develop into the medium. For example, in Fig. 6(a), when  $\omega$  corresponds to  $k_1, k_2$ , and  $k_3$ , only  $k_1$  could be selected. In this case,  $k_2$  has a locally negative group velocity so that it cannot propagate forward. Although the tangent slope at  $k_3$  is positive, it is not able to “push” the propagation of all the modes of  $k < k_3$  since the line AB has a negative slope.

In fact, all dispersion curves are not monotonic if we add its mirror part at  $k < 0$ . When dispersion is negative ( $d\omega/d|k| < 0$ ) as in Fig. 2(c), negative  $k$  gives positive  $V_g$  while positive  $k$  gives negative  $V_g$  [Fig. 6(b)]. Forced by any frequency within the scope of the dispersion curve, the system chooses a mode with  $k < 0$ , so we see counterpropagating waves [Fig. 6(c)]. The necessary and sufficient condition for counterpropagating waves should then be stated as: the forcing frequency  $\omega$  is lower than the frequency of bulk oscillation and also within the scope of the dispersion curve. No matter whether the dispersion is monotonic or not, such a condition ensures that at least one corresponding mode  $[k(<0), \omega]$  with positive tangent’s slope exists. Among them, the system will select the point with the smallest  $|k|$  since the other points must have plot lines with negative slope.

As to 2D antispirals, the organizing center acts as a wave source with a specific frequency  $\Omega_{AS}$ . From the conclusion above, we get  $\Omega_{AS} < \Omega_0$  as a criterium of antispirals. Another criterium  $\frac{d\omega}{d|k|}|_{|k|} < 0$  is also implied in it since the system selects the only mode with positive group velocity  $\frac{d\omega}{dk}|_k > 0$ .

The frequency  $\Omega_{AS}$  is usually a medial value on the dispersion curve but hard to predict. However, we could give a necessary condition, which may help predict the occurrence of antispirals: the dispersion should be generally negative, which means that the bulk oscillation frequency should be relatively high (at least not the lowest) on the dispersion curve so as to permit a source mode with a frequency lower than it. This kind of dispersion is possibly found in relaxational oscillatory media just as we conceived, so antispirals may exist in oscillatory media no matter whether the system is close to or far from Hopf onset. When we deduce group velocity, we have agreed there are no sharp differences between oscillatory and excitable media so that we can discuss them in one theoretical scheme. However, the dispersion of an excitable medium displays a notable quality: the bulk oscillation frequency is equal to zero so that the bulk mode lays at the lowest point of the dispersion curve. Since this general quality of excitable media disobeys the necessary condition above of antispirals, we conclude that antispirals cannot exist in excitable media.

#### ACKNOWLEDGMENTS

This work is partially supported by the Chinese Natural Science Foundation, the Department of Science and Technology of China. C.W. thanks the Jun-Zheng Foundation at PKU.

- [1] M. C. Cross and P. C. Hohenberg, *Rev. Mod. Phys.* **65**, 851 (1993).  
 [2] A. T. Winfree, *Chaos* **1**, 303 (1991).  
 [3] V. K. Vanag and I. R. Epstein, *Science* **294**, 835 (2001).  
 [4] V. K. Vanag and I. R. Epstein, *Phys. Rev. Lett.* **87**, 228301 (2001).  
 [5] E. M. Nicola, L. Bruschi, and M. Bär, *J. Phys. Chem. B* **108**,

- 14733 (2004).  
 [6] Y. Gong and D. J. Christini, *Phys. Rev. Lett.* **90**, 088302 (2003).  
 [7] H. Skødt and P. G. Sørensen, *Phys. Rev. E* **68**, 020902(R) (2003).  
 [8] S. J. Woo, J. Lee, and K. J. Lee, *Phys. Rev. E* **68**, 016208 (2003).

- [9] J. Davidsen, L. Glass, and R. Kapral, Phys. Rev. E **70**, 056203 (2004).
- [10] A. M. Pertsov, M. Wellner, and J. Jalife, Phys. Rev. Lett. **78**, 2656 (1997).
- [11] M. Wellner and A. M. Pertsov, Phys. Rev. E **55**, 7656 (1997).
- [12] V. K. Vanag and I. R. Epstein, Phys. Rev. Lett. **88**, 088303 (2002).
- [13] M. Stich and A. S. Mikhailov, J. Phys. Chem. **216**, 521 (2002).
- [14] V. Duffiet and J. Boissonade, J. Chem. Phys. **96**, 664 (1992).
- [15] L. Brillouin, *Wave Propagating and Group Velocity* (Academic, New York, 1960).
- [16] G. B. Whitham, Proc. R. Soc. London, Ser. A **283**, 238 (1965).
- [17] M. J. Lighthill, J. Inst. Math. Appl. **1**, 1 (1965).
- [18] C. D. Decker and W. B. Mori, Phys. Rev. Lett. **72**, 490 (1994).
- [19] D. Walgraef, Phys. Rev. E **55**, 6887 (1997).
- [20] D. Barkley, M. Kness, and L. S. Tuckerman, Phys. Rev. A **42**, 2489 (1990).
- [21] We measure the oscillatory frequency during a small period of time  $\Delta t$  ( $\Delta t \ll t_{n+1} - t_n$ ) at each spatial point to determine the temporary  $\omega \sim x$  curve.